Towards the selective fixation of palladium on composite oxide carriers

A. Bensalem, G.A. Shafeev and F. Bozon-Verduraz [1]

Laboratoire de Chimie des Matériaux Divisés et Catalyse, Université Paris 7 (Denis Diderot), 2, place Jussieu, 75251 Paris Cedex 05, France

Received 13 June 1995; accepted 13 November 1995

The selective metallization of a semiconducting oxide (ceria) supported on an insulating oxide (silica) is investigated through new methods involving optical and electronic properties of the components of the composite. Supported ceria particles in the nanometer range are studied. Two methods of Pd deposition are applied: (i) electroless deposition via laser activation of the composite suspension in the Pd precursor solution; (ii) UV photoreduction of Pd on the composite. Electroless deposition results in a wide distribution of metal particle size, from 2–3 nm to 600 nm, while some ceria particles are not metallized at all. On the contrary, photoreduction fixes the Pd on ceria selectively, yielding Pd particles with sizes comparable to that of the ceria. The influence of various parameters governing the metal deposition is discussed.

Keywords: palladium–ceria–silica catalysts; electroless deposition; photodeposition

1. Introduction

During the last three decades, numerous studies were devoted to the influence of metal–support interactions on the activity and selectivity of metal catalysts [1,2]. Even though the respective roles of the metal particle size and of the properties (acid–base and redox) of the carrier could not be clearly separated, some interesting trends were evidenced. For example, the use of basic carriers in Pd catalysts was shown to favour the production of oxygenates from $CO + H_2$ reaction mixtures [3,4]. The modification of the properties of the carrier need not be limited to changing the carrier itself; it can also be done through: (i) introduction of *additives*, an old practise; (ii) the use of *composite* oxides. The latter method has recently received increased attention especially in the papers by Schwarz et al. [5] who have tried to carry out the selective fixation of a metal on just one component of the composite. The procedure developed by these authors is based on the different exchange abilities of the two oxide phases, which arise from their different points of zero charge (PZC). However, this method seems to be useful only when the disparity of the PZC is large. Moreover, while modifications in the catalytic behaviour have been established [6], the location of the metal in the composite has not. We propose another approach to achieve the selective fixation of a metal on one component of a composite when that component is semiconducting (s.c.) and the other is an insulator. This approach exploits the differences in electronic and optical properties of each oxide, the semiconducting being susceptible to *photoactivation*. In the present work, two procedures are applied: *electroless plating* and *photoassisted reduction*.

Electroless plating is an ancient procedure [7] which has lately received renewed attention, in particular in the field of microelectronics [8]. This method has been applied recently in the preparation of supported metal catalysts [9].

Photoassisted reduction is a well-known process which has been applied to the preparation of monometallic and bi-metallic catalysts but, up to now, these investigations have concerned exclusively *bulk* semiconductors [10–15].

The selective fixation of a metal on *nanoparticles* of a supported oxide offers two points of interest: (i) an increase of the number of metal atoms interacting with this oxide, (ii) study of the influence of the oxide particle size, and hence of its *coordinative unsaturation*, on the metal–oxide interaction. It implies that well characterized highly dispersed oxide samples are available. We decided to start this study with CeO_2, an n-type semiconducting oxide because of its importance in automotive exhaust catalysts. Silica, alumina and magnesia were selected as the major components of the carrier, since they are all insulating and present large differences in acid–base properties. The present work focuses on CeO_2–SiO_2 systems, which have been well characterized in our laboratory [16]. Investigations on CeO_2–Al_2O_3 and CeO_2–MgO are now in progress.

2. Experimental

Silica-supported ceria was prepared according to a procedure described elsewhere [16] from Degussa Aerosil (specific surface 340 m^2/g) and cerium(IV) acetylacetonate. Two classes of CeO_2/SiO_2 samples were used (table 1). A standard Pd electroless solution was used with palladium tetrammine chloride as a metal source and hydrazine hydrate N_2H_4 as a reducing agent [7] similar to that used earlier for the metallization of bulk ceria

[1] To whom correspondence should be addressed.

Table 1
Characterization of composite oxides

Sample	CeO_2 (%)	Average particle size (nm)	Surface area (m^2/g)
COS 23	13.3	4.5–8.5	237
COS 16	9.8	1–3	246

[9]. A 1 g aliquot of the composite containing the larger particles of ceria (COS23) was immersed into the electroless solution. The stirred suspension was irradiated in a quartz cell with an excimer XeCl laser ($\lambda = 308$ nm, 60 mJ/pulse, repetition rate 1 Hz, pulse duration 30 ns) during 10 min. The solid obtained after the reaction was rinsed many times in distilled water and dried. The Pd content was determined by inductively coupled plasma emission spectroscopy.

In the case of photodeposition, the composite powder was dipped into the solution of the Pd precursor (0.5 g of COS16 for 100 cm^3). Two kinds of solutions were used: (i) a solution of palladium tetrammine (3.7×10^{-3} M) at pH = 10; (ii) a solution of palladium nitrate (5×10^{-5} M) in a slightly acidic (pH = 5) 1 : 1 mixture of water and isopropanol. The continuously stirred suspension was irradiated with a high-pressure mercury lamp (Hanovia, 200 W) during 6 h.

X-ray photoelectron spectra (XPS) were recorded on an ESCA 3 Mark III equipment with an Al Kα source (200 W, 1486.6 eV). Energy referencing was carried out with the Si 2p peak of silica at 103.5 eV [17]. STEM experiments were performed on a VG HP5 scanning transmission electron microscope equipped with an energy dispersive X-ray analyser (X-EDS).

3. Results and discussion

3.1. Electroless plating of palladium assisted by laser irradiation

3.1.1. Preliminary remarks

Electroless plating is a mixed potential reaction consisting of the anodic oxidation of a reducing agent and the cathodic reduction of the metal precursor. The electrons are transferred from the reducing agent to the metal ion via the surface sites of a solid substrate. When using a dielectric substrate, a catalytic procedure is believed to be necessary for electroless deposition [8] and the catalytic sites may be atomic defects created by irradiation [9,18]. Laser irradiation of the composite powder serves to activate selectively ceria particles for electroless plating.

Without laser irradiation, no Pd deposition was observed after several hours at ambient temperature, both with CeO_2/SiO_2 powder (COS 23) and pure silica.

With laser irradiation, the suspension becomes very rapidly grey indicating the onset of deposition. The corresponding reaction may be written:

$$2Pd(NH_3)_4^{2+} + N_2H_4 + 4OH^- \rightarrow 2Pd^0 + 8NH_3 + N_2 + 4H_2O \quad (1)$$

The Pd content of the metallized composite is 3.6%.

3.1.2. XPS analysis

The Pd $3d_{3/2}$ and $3d_{5/2}$ peaks appear at 340.3 and 335.2 eV respectively (fig. 1A). These binding energies correspond to metallic Pd [19–23].

3.1.3. STEM analysis

Examination of Pd/ceria catalysts presents particular difficulties because of poor contrast and discrimination between the two components requires X-EDS analysis.

As shown in table 2, the samples contain: (a) numerous small particles with weak contrast showing similar Pd and Ce surface loadings; (b) medium size cerium-rich particles where Pd is sometimes scarcely detectable; (c) some very large palladium-rich particles (appearing as monocrystalline on the pictures, not shown) showing some contrast which means that Pd is located on both silica and ceria. It may be concluded that uncontrolled growth of palladium occurred in (c) whereas the palladium deposition was selective and controlled in (a), (b) showing the presence of uncovered ceria particles.

3.1.4. Discussion

The results presented above involve the catalytic reduction of Pd^{2+} ions, which forms Pd^0 nuclei. The rate of the electroless deposition is governed by the rate of the oxidation of the reducing agent [8]. This oxidation may occur both on the activated dielectric surface and

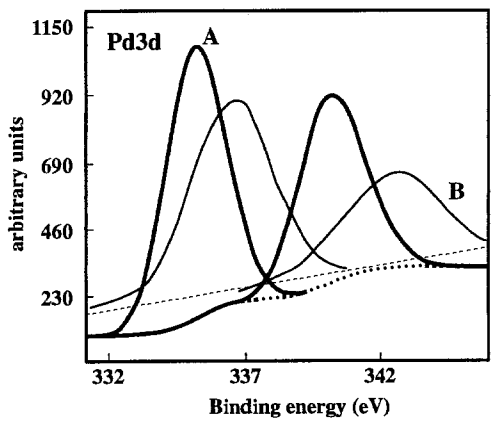

Fig. 1. X-ray photoelectron spectra of (A) 3.63% Pd/CeO_2–SiO_2 prepared by electroless deposition, (B) 1.20% Pd/CeO_2–SiO_2 prepared by photodeposition in slightly acidic medium. Full line: smoothed spectrum; broken line: Shirley background.

Table 2
Sample prepared by electroless deposition

Area	Size (nm)	Si (%)	Ce (%)	Pd (%)
(a)	2–3	88.0	3.5	8.5
(a)	2–3	84.8	5.6	9.6
(a)	2–3	82.7	4.9	12.5
(a)	2–3	87.8	4.0	8.3
(a)	2–3	86.8	4.7	8.5
(a)	4	69.7	26.7	3.6
(a)	5	81.8	4.0	14.2
(b)	10	44.2	52.5	3.2
(b)	10	48.0	49.2	2.9
(b)	10	41.8	58.2	–[a]
(b)	12	24.3	75.7	–[a]
(b)	16	63.3	34.0	2.7
(c)	150	39.9	12.6	47.5
(c)	250	1.6	–[a]	98.4
(c)	300	44.2	11.6	44.2
(c)	600	32.8	11.0	56.2

[a] Not detected.

on the deposited metal. However, the oxidation proceeds much faster in the vicinity of the metal since the density of electronic states around the electrochemical potential of oxidation of the reducing agent is much higher in the case of metal surface than in the case of the activated dielectric, whatever the activation method. In addition, whereas the dielectric sites are equivalent in the early stages of deposition, there is a critical radius for a metal cluster to induce the electroless deposition, around 10 atoms [8]. Once the deposition starts, the reaction rate is proportional to the metal particle surface. This means that large metal particles grow faster than small ones. For this reason, there are very few large clusters of metal (150–600 nm) whereas some dielectric sites are not metallized at all. It follows that the metal distribution is heterogeneous and non-selective. Hence the electroless procedure produces a wide distribution of particle size while some ceria sites remain metal-free until the end of the reaction.

Laser-assisted activation of electroless deposition of metal is a multistep phenomenon. The selectivity of the deposition depends on various factors. First, the fast heating of ceria induced by laser radiation may result in the formation of dielectric catalytic sites, as it was shown previously for bulk ceria [9]. Second, the intense UV irradiation creates electron–hole pairs in ceria (see below the section on photodeposition). The photoelectron may reduce the adsorbed Pd ions to Pd^0 nuclei which are efficient sites for electroless deposition.

3.2. Photodeposition of palladium

In this section, the composite oxide with smaller ceria particles (COS16) was used.

3.2.1. Preliminary remarks

The photodeposition occurs when a semiconducting carrier is illuminated with photons of energy $E > E_g$ (band gap width) in the presence of the metal precursor in solution. The reduction of the metal cation is achieved by the electrons produced under illumination provided that the associated holes are rapidly consumed by the reaction medium. Various types of alcohols may serve as hole scavengers [10].

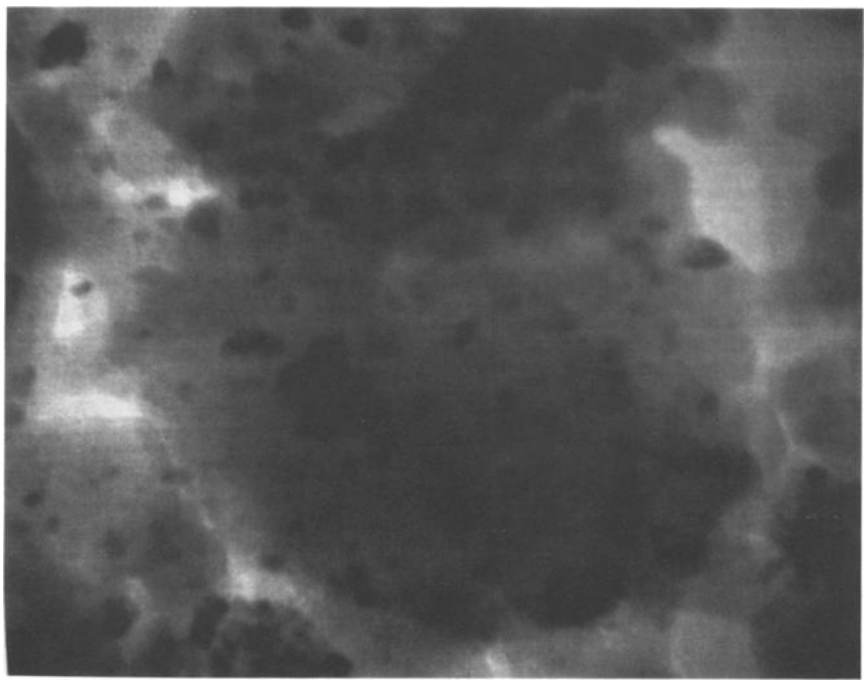

Fig. 2. STEM picture of Pd/CeO_2–SiO_2 prepared by electroless deposition.

3.2.2. Photodeposition in basic medium (pH > 9)

The initially colorless suspension of composite in palladium tetrammine becomes slightly grey after 6 h exposure to UV radiation. XPS analysis of the powder obtained (Pd content = 1.96%) shows that the binding energies amount to about 338.3 eV for Pd $3d_{5/2}$ and 343.9 eV for Pd $3d_{3/2}$, which shows only the presence of Pd^{2+} [19,22,23].

3.2.3. Photodeposition in slightly acidic medium (pH = 2–5)

In this set of experiments isopropanol was used as a hole scavenger and Pd nitrate as a precursor. The suspension becomes grey after 30 min of irradiation and the saturation is achieved within 3–4 h. The Pd content in the powder obtained after filtration and drying is 1.2%.

XPS analysis. The spectra of Pd (fig. 1B) show two abnormally large peaks centered respectively at 336.4 eV ($3d_{5/2}$) and at 342.2 eV ($3d_{3/2}$). Their binding energies (BE) are intermediate between the BE of Pd^0 and the BE reported for Pd^{2+}, that is for the peak $3d_{5/2}$: (i) $335.1 < BE < 335.8$ eV for Pd^0 [20,22], (ii) $BE > 337.0$ eV for Pd^{2+} [19–23]. On the other hand, metallic Pd is clearly identified by X-ray diffraction and STEM analysis (see below). Hence the peaks at 336.4 and 342.2 eV are ascribed to metallic Pd in interaction with residual Pd^{2+} ions.

STEM analysis. In this sample (table 3), palladium and cerium were always detected together and the Pd/Ce ratio increases with the particle size. It follows: (i) that palladium was deposited onto ceria particles; (ii) metal growth was limited (fig. 3).

Table 3
Sample prepared by photodeposition

Size (nm)	Si (%)	Ce (%)	Pd (%)
3	66.2	14.6	19.2
3	76.1	18.1	5.9
3	83.0	10.6	6.5
6	54.6	12.0	33.5
6	54.3	8.9	36.8
8	54.6	12.0	33.5
8	47.5	11.9	40.6
10	46.3	5.8	47.9
10	54.3	9.2	36.6
12	48.6	3.9	47.5
20	25.7	41.7	32.6
40	42.3	5.5	52.2
40	16.6	2.4	81.0

3.2.4. Discussion

It appears that the photoreduction of Pd in a slightly acidic medium results in selective deposition of the metal onto ceria nanoparticles. There are traces of unreduced Pd on the support; on the other hand, when starting from a basic solution, the photoreduction does not occur. It is worthwhile to note that the pH of the precursor solution plays a crucial role. First, at lower initial pH, ceria particles may be dissolved by the solution, and the quantity of deposited Pd would then be very small since there would be not enough solid ceria to be photoactivated. This is why intermediate and high pH values were first selected in the present work. However, at high pH (> 9), Pd^{2+} can precipitate as $Pd(OH)_2$, which may deposit unselectively on the composite carrier, leading to the decrease of the Pd^{2+} concentration and, consequently, to

Fig. 3. STEM picture of Pd/CeO_2–SiO_2 prepared by photodeposition.

a drop of the oxidation potential E. At intermediate pH, no precipitation occurs but E still depends on the nature of the predominant Pd^{2+} species. On the other hand, the pH of the solution increases upon irradiation; for instance, during 1.5 h of irradiation of the suspension, the pH changes from 2.7 (initial value) to 4.3 (end of deposition). Similar experiments performed on pure (unsupported) ceria show also an increase of pH, which is enhanced when the initial pH is changed from 2.1 to 3.2 (fig. 4). This result may explain the presence of Pd^{2+} in the experiments carried out at an initial pH = 5. If the pH of the solution becomes > 8, the Pd ions may precipitate and generate a thin hydroxide coating on the palladium metal previously deposed. The increase of pH upon irradiation can be explained by the photoreduction of H^+ ions to hydrogen atoms.

Hydrogen atoms adsorbed on ceria may then either recombine to yield gaseous H_2 or reduce Ce^{4+} ions to Ce^{3+}, leading to the partial reduction of the supported oxide. During the deposition, the concentration of Pd^{2+} complexes decreases continuously and so does the electrochemical potential of the Pd^{2+}/Pd couple. When the Pd^{2+} concentration is low enough, the reduction of H^+ ions is favoured, which explains the emission of gas bubbles at the end of Pd reduction.

On the other hand, the first Pd nucleus deposited onto ceria acts as a cathode, while the ceria itself becomes an anode, as suggested previously for the Pt/TiO_2 system [10]; this microcell enhances the deposition rate, which leads to the formation of Pd particles larger than ceria particles.

4. Conclusion

Palladium deposition on *composite* ceria–silica powders has been performed using laser-assisted electroless deposition and UV photoreduction, taking into account the differences in electronic and optical properties of the two oxides (semiconducting ceria and insulating silica).

Palladium deposited via the *electroless procedure* is detected exclusively in the metallic form. On the other hand, the distribution of size of Pd particles is very large. Along with small particles (2–3 nm), there are also big ensembles (150–600 nm), while some ceria particles are not metallized at all. This is ascribed to a very rapid growth on metallic particles compared to a slow one on the dielectric sites. It appears that electroless deposition is not convenient to obtain narrow particle size distributions on dielectric particles.

On the other hand, Pd deposition via *UV assisted photoreduction* is better suited for controlling the location of metal particle and their range of size. No Pd-free ceria particles have been found. Among the parameters governing the photoreduction of Pd, the pH value of the precursor solution seems to be the most important. Its control maintains the (Pd^{2+}/Pd) potential below the level of the ceria conduction band, a prerequisite to the photoreduction [15,24]; it also precludes the precipitation of palladium hydroxide, taking into account the pH increase arising from the photoreduction of adsorbed H^+ ions. The best results are obtained in slightly acidic medium (pH ≈ 3–5). Such a selective metallization method may be extended to any composite system containing a semiconducting phase fixed on an insulating support. Investigations on ceria–alumina and ceria–magnesia composites are now in progress.

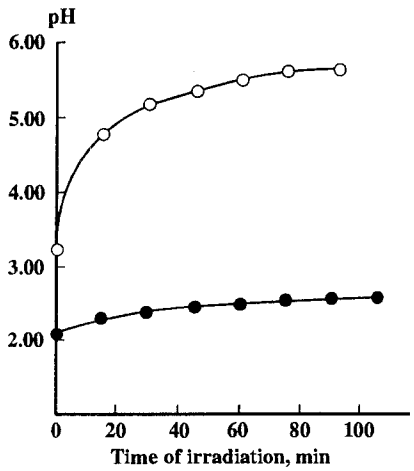

Fig. 4. pH variation of a ceria suspension against irradiation time: initial pH: 2.1 (full circles), 3.2 (open circles).

Acknowledgement

Contributions of Mrs. E. Merlen (from Institut Francais du Pétrole) for STEM-EDX measurements, of M.M. Leclerc (Université Paris 7-Denis Diderot) for XPS experiments and of M.A. Ensuque (Université Paris 7-Denis Diderot) were greatly appreciated.

References

[1] *Metal–Support and Metal–Additives Effect in Catalysis*, Stud. Surf. Sci. Catal. 11 (1982).
[2] A.M. Vannice, J. Mol. Catal. 165 (1990) 165.
[3] V. Ponec, *New Trends in CO Activation*, Stud. Surf. Sci. Catal. 64 (1991) 117.
[4] P. Hindermann, G.J. Hutchings and A. Kiennemann, Catal. Rev. Sci. Eng. 35 (1993) 1.
[5] J.A. Schwarz, Catal. Today 15 (1992) 395.
[6] R. Zhang, J.A. Schwartz, A. Datye and J.P. Baltrus, J. Catal. 135 (1992) 200.
[7] G. Gutzeit, E.B. Saubestre and D.R. Turner, *Electroplating Engineering Handbook*, ed. A.K. Graham, 3rd Ed. (Van Nostrand, New York, 1971);
W.A. McRae, in: *Kirk Othmer Encyclopedia of Chemical Technology*, 3rd Ed., Vol. 8 (1979) p. 738.
[8] M. Paunovic and J. Ohno, *Proc. Symp. Electroless Deposition of Metals and Alloys* (The Electrochemical Society, Pennington, 1988).

[9] A. Bensalem, G. Shafeev and F. Bozon-Verduraz, Catal. Lett. 18 (1993) 165.
[10] A. Fernandez, G. Munuera, A.R. Gonzalez-Elipe and J.P. Espinoz, Appl. Catal. 57 (1990) 151.
[11] J.M. Herrmann, J. Disdier, P. Pichat, A. Fernandez, A. Gonzalez-Elipe, G. Munuera and C. Leclercq, J. Catal. 132 (1991) 490.
[12] S. Shinri, J. Catal. 92 (1985) 11.
[13] J.M. Herrmann, J. Disdier and P. Pichat, J. Catal. 113 (1988) 72.
[14] K.H. Stadler and H.P. Boehm, in: *Proc. 8th Int. Congr. on Catalysis*, Berlin, Vol. IV (Dechema, Frankfurt-am-Main ,1984) p. 803.
[15] F. Moller, H.J. Tolle and R. Memming, J. Electrochem. Soc. 121 (1974) 1160.
[16] A. Bensalem, F. Bozon-Verduraz, M. Delamar and G. Bugli, Appl. Catal. A 121 (1994) 81.
[17] C.D. Wagner, in: *Practical Surface Analysis by Auger and X-Ray Photoelectron Spectroscopy*, Vol. 1, eds. D. Briggs and M.P. Seah (Wiley, Chichester, 1990) app. 5, p. 595.
[18] G.A. Shafeev, Adv. Mater. Optics Electron. 2 (1993) 183.
[19] F. Bozon-Verduraz, A. Omar, J. Escard and B. Pontvianne, J. Catal. 53 (1978) 126.
[20] M. Narayana, J. Michalik, S. Contarini and L. Kevan, J. Phys. Chem. 89 (1985) 3895.
[21] A.Y. Stakheev and W.H.M. Sachtler, J. Chem. Faraday Trans. 87 (1991) 3703.
[22] G. Kumar, J.R. Blackburn, W.E. Modderman, R.G. Albridge and M.M. Jones, Inorg. Chem. 11 (1972) 296.
[23] K. Kim, A. Gossmann and N. Winograd, Anal. Chem. 46 (1974) 197.
[24] M. Grätzel, *Photocatalysis, Fundamentals and Applications*, eds. Serpone and Pelizzetti (Wiley, New York, 1989) p. 123.